Electronic Supplementary Material (ESI) for Journal of Materials Chemistry A.

Electronic Supplementary Information

Sandwiched C@SnO_2@C Hollow Nanostructures as an Ultralong-Lifespan High-Rate Anode Material for Lithium-Ion and Sodium-Ion Batteries

Jian Qin,[a] Naiqin Zhao,[a, b] Chunsheng Shi,[a] Enzuo Liu,[a, b] Fang He,[a] Liying Ma,[a] Qunying Li,[a] Jiajun Li,[a] and Chunnian He* [a, b]

[a] School of Materials Science and Engineering and Tianjin Key Laboratory of Composites and Functional Materials, Tianjin University, Tianjin, 300072, P. R. China

[b] Collaborative Innovation Center of Chemical Science and Engineering, Tianjin 300072, China

* Address correspondence to

cnhe08@tju.edu.cn

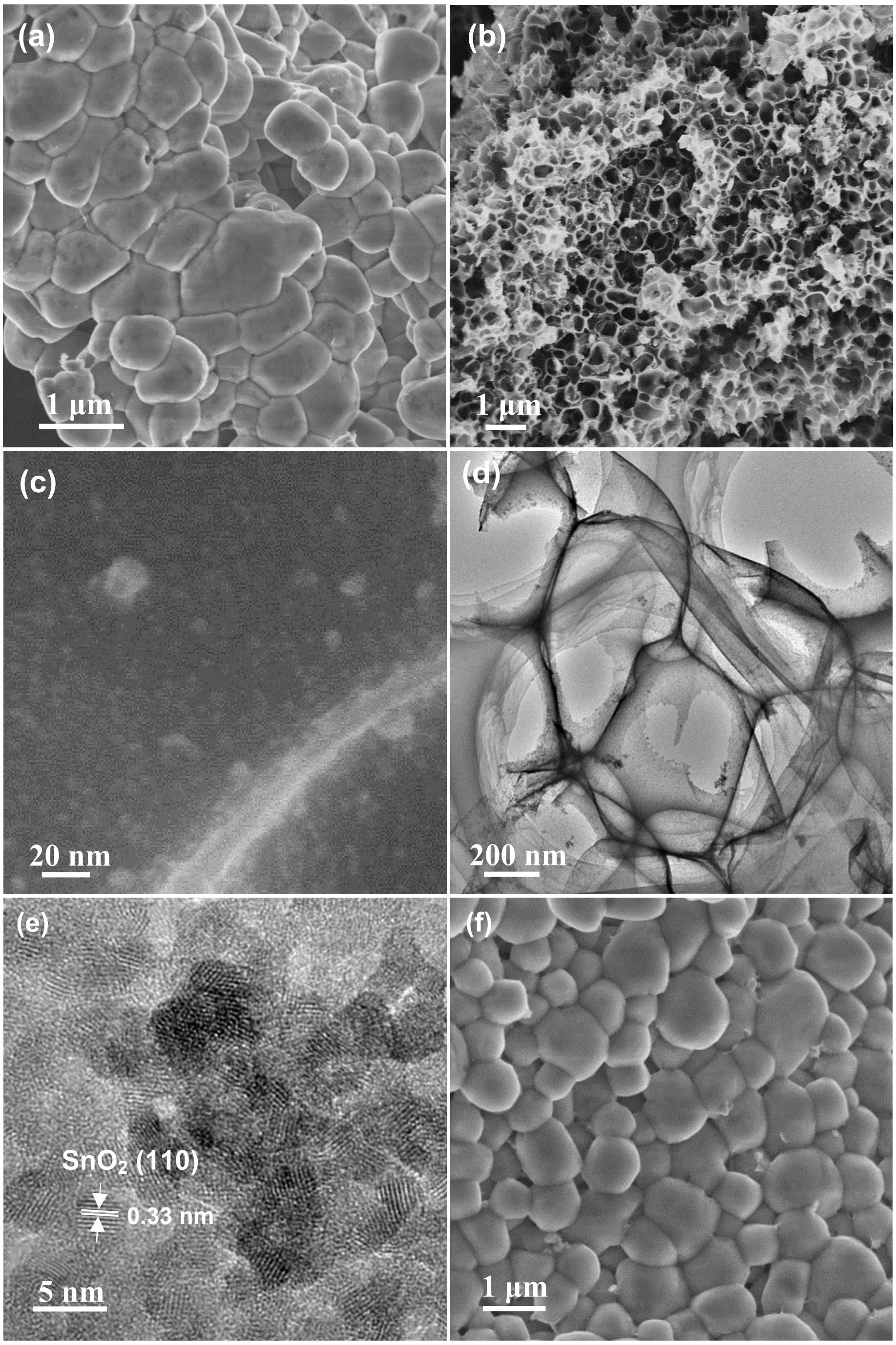

Fig. S1. (a) A typical SEM image of the 3D interconnected NaCl cubes coated with uniform thin film of $SnCl_4$-$C_6H_8O_7$ complex after freeze-drying process. (b)-(c) SEM and (d)-(e) TEM images of 3D porous carbon networks homogeneously anchored with numerous ultrasmall SnO_2 nanocrystals of 2~5 nm (denoted with C@SnO_2 composites) after removing NaCl but before the CVD carbon coating process. Note that the C@SnO_2 composite does not display perfectly pore structure because of some defects and fractures resulting from structural collapses of the NaCl template during the carbonization or template removal process. (g) A typical SEM image of 3D interconnected NaCl particles coated with C@SnO_2@C (NaCl@C@SnO_2@C) before eliminating the NaCl template.

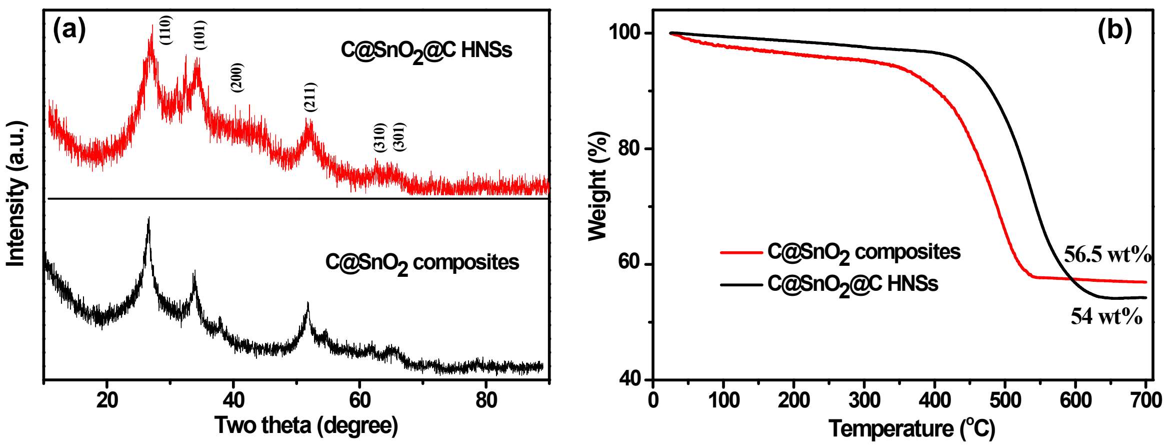

Fig. S2. (a) XRD patterns and (b) TGA profile of C@SnO_2@C HNSs and C@SnO_2 composite. It can be seen that the diffraction peaks of C@SnO_2 composites can be well indexed to the tetragonal SnO_2 phase (JCPDS 41-1445) and the C@SnO_2 composites contains 43.5 wt.% carbon without the CVD carbon coating process.

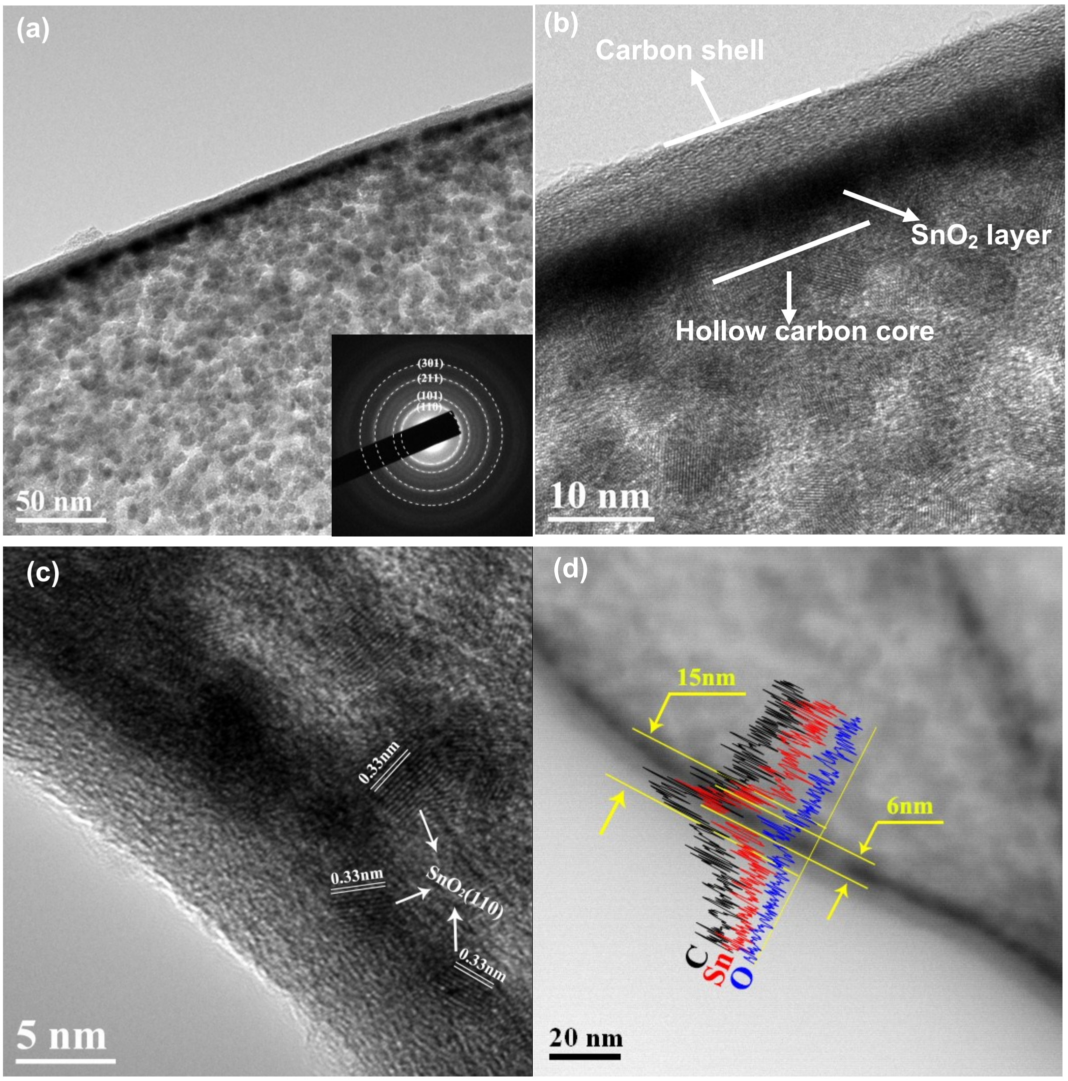

Fig. S3. (a) TEM image and SEAD pattern, (b, c) HRTEM images, (d) elemental line scanning image of the C@SnO_2@C HNSs composite, in which a definite composition order of the shells is confirmed. The outer carbon shell, which derived from the CVD of C_2H_2, shows a clear profile both in HRTEM and elemental line scanning images and its thickness is about 5 nm. The interbedded SnO_2 layer with a thickness of about 6 nm is composed of numerous ultrasmall SnO_2 nanocrystals. The inner hollow carbon core, which derived from the pyrolysis of solid carbon source (citric acid), can be recognized from the C element line scanning image in Fig. S3d and its thickness is about 4 nm.

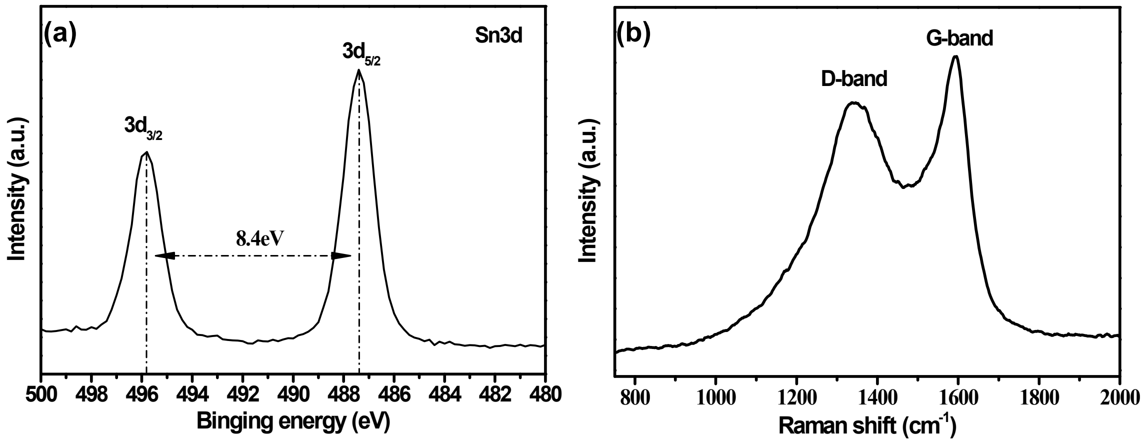

Fig. S4. (a) XPS spectra of Sn3d peaks and (b) Raman spectrum of $C@SnO_2@C$ HNSs.

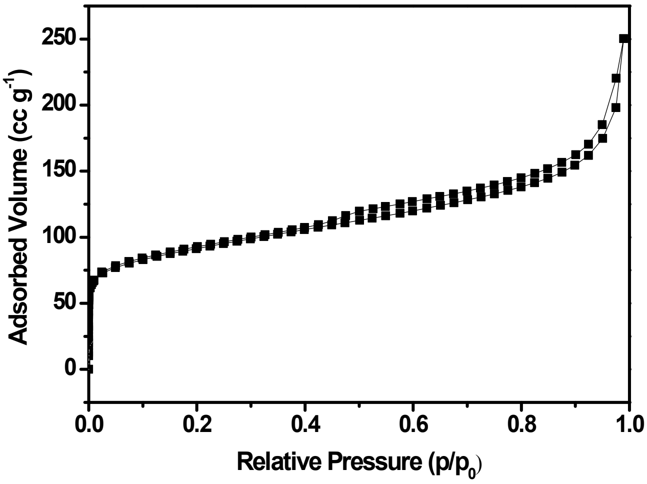

Fig. S5. Nitrogen adsorption–desorption isotherms of $C@SnO_2$ composites.

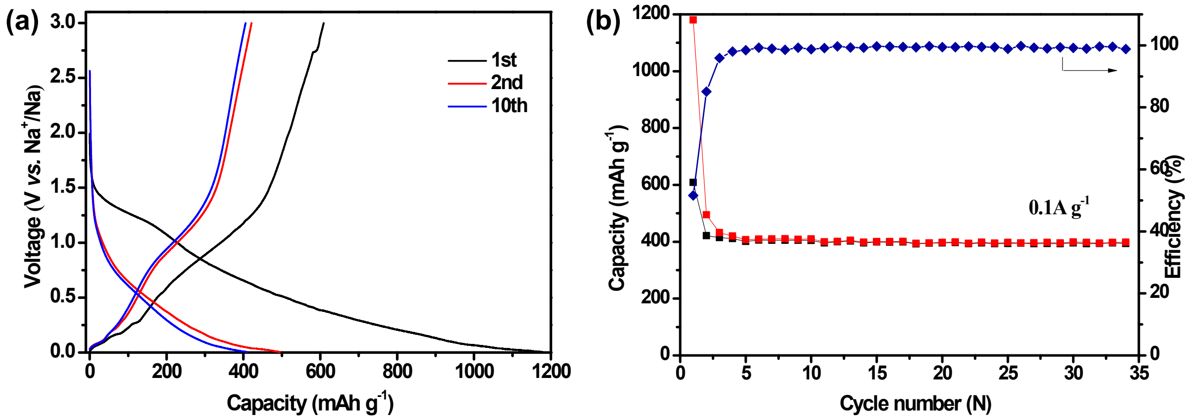

Fig. S6. (a) Galvanostatic charge−discharge voltage profiles plotted for the first, second and 10th cycles of the C@SnO_2@C HNS electrode for SIB anode at a current density of 0.1 A g^{-1}. (b) Cycling performance of the C@SnO_2@C HNS electrode for SIB anode at a current density of 0.1 A g^{-1}.

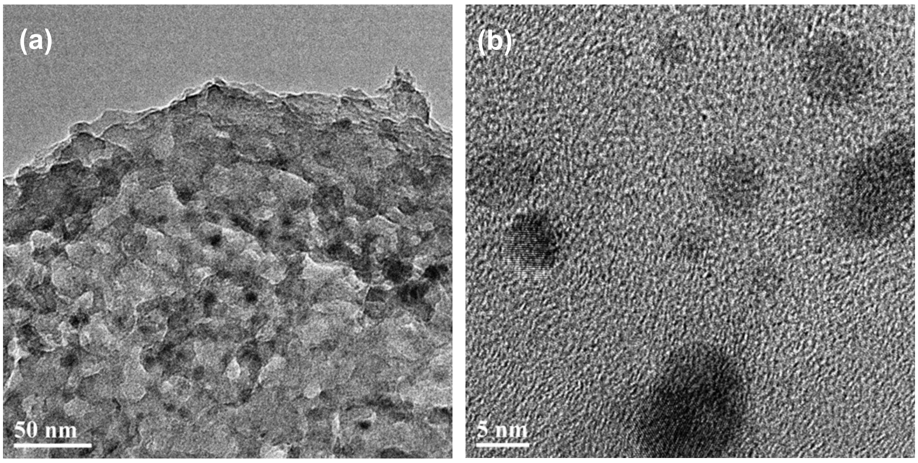

Fig. S7. (a) TEM and (b) HRTEM image of C@SnO_2@C HNSs as a LIB anode after 1000 cycles at 10 A g^{-1}.

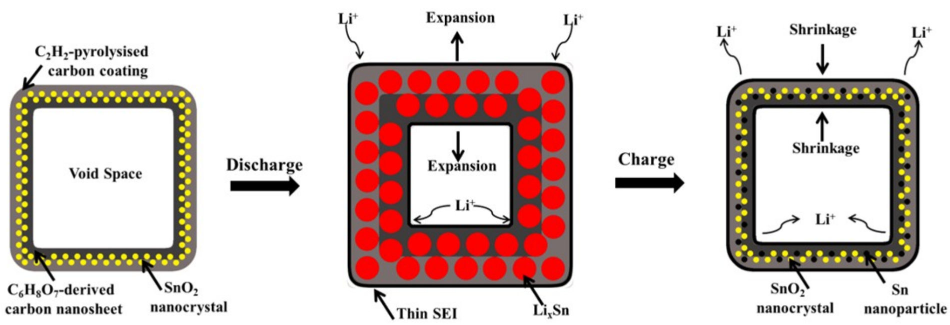

Fig. S8. Schematic illustration of a C@SnO_2@C HNS for lithium storage processes. Sodium storage processes of the nanostructures like the case of lithium storage processes.

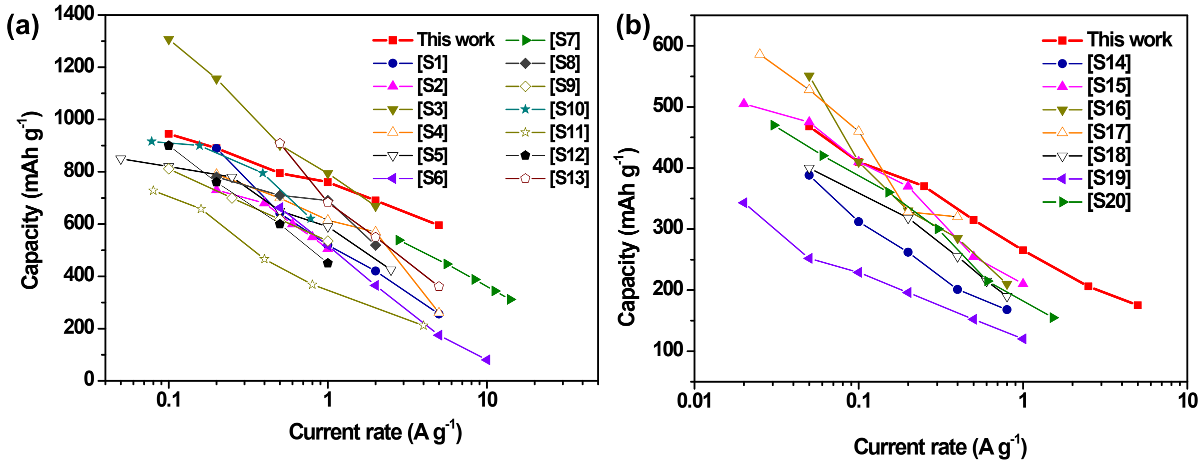

Fig. S9. (a) Comparison of rate capacity of C@SnO_2@C HNS electrode for LIB anode with those of representative SnO_2/C composite anodes previously reported. (b) (a) Comparison of rate capacity of C@SnO_2@C HNS electrode for SIB anode with those of representative SnO_2/C composite anodes previously reported.

Table S1. Comparison of specific lithium storage capacity and capacity retention at different current densities for C@SnO_2@C HNS electrode with those of the representative previously reported SnO_2/C composite anodes.

Materials	Current density (A g^{-1})	Cycle number	Specific capacity (mAh g^{-1})	Capacity retention (%)
C@SnO_2@C HNSs [this work]	**0.1**	**50**	**933**	**92**
	5	**1000**	**550**	**95**
	10	**1000**	**285**	**92**
Carbon-coated SnO_2 submicroboxes [S1]	0.5	100	491	50
Carbon-coated SnO_2 nanoplates [S2]	0.2	50	700	80
Carbon-coated hierarchical	0.1	50	920	75

SnO_2 hollow spheres[S3]				
2D graphene/ SnO_2@C[S4]	0.2	100	800	90
Carbon-encapsulated porous SnO_2[S5]	0.5	200	516	81
SnOx/carbon nanohybrids [S6]	0.5	200	608	86
Ultrasmall SnO_2 confined in micro/mesoporous carbon [S7]	1.4	2000	443	75
SnO_2/graphene composites [S8]	0.1	200	872	85
Reduced GO/SnO_2 nanocomposites [S9]	0.1	200	718	72
	0.5	200	514	70
Graphene-based mesoporous SnO_2 composite [S10]	0.782	50	847.5	78
Graphene/SnO_2 composite [S11]	0.08	120	591.9	60
SnO_2@C nanocomposites [S12]	0.1	200	880	86
SnO_2/carbon nanotubes [S13]	0.5	200	602	64

Table S2. Comparison of specific sodium storage capacity and capacity retention at different current densities for C@SnO_2@C HNSs electrode with those of representative SnO_2/carbon composite anodes reported previously.

Materials	Current density ($A\ g^{-1}$)	Cycle number	Specific capacity ($mAh\ g^{-1}$)	Capacity retention (%)
C@SnO_2@C HNSs [this work]	**0.1**	**30**	**405**	**97%**
	4.6	**3000**	**200**	**90**
SnO_2/graphene composites [S14]	0.05	70	297	79

SnO_2 particles dispersed between graphene nanosheets [S15]	0.5	100	260	82
SnO_2 nanoparticles embedded in 3D graphene [S16]	0.1	200	432	85.7
SnO_2@N-doped carbon@SnO_2 nanotubes [S17]	0.025	50	492	72
SnO_2@void@C porous nanowires [S18]	0.2	100	308	83
Sn/SnO_2/C composites [S19]	0.02	100	245	78
Carbon encapsulated SnO_2 nanocomposites [S20]	0.152	200	360	80

References

[S1] X. S. Zhou, L. Yu, X. W. Lou, *Adv. Energy Mater.* **2016**, 1600451.

[S2] L. Zhang, G. Zhang, H. Wu, L. Yu, X. Lou, *Adv. Mater.* **2013**, *25*, 2589.

[S3] Q. N. Liu, Y. H. Dou, B. Y. Ruan, Z. Q. Sun, S. L. Chou, S. X. Dou. *Chem. Eur. J.* **2016**, *22*, 5853.

[S4] Y. Su, S. Li, D. Wu, F. Zhang, H. Liang, P. Gao, C. Cheng, X. Feng, *ACS Nano* **2012**, *6*, 8349.

[S5] B. Huang, X. H. Li, Y. Pei, S. Li, X. Cao, R. C. Massé, G. Z. Cao, *Small* **2016**, *12*, 1945.

[S6] X. S. Zhou, Z. H. Dai, S. H. Liu, J. C. Bao, Y. G. Guo, *Adv. Mater.* **2014**, *26*, 3943.

[S7] A. Jahel, C. M. Ghimbeu, L. Monconduit, C. Vix-Guterl, *Adv. Energy Mater.* **2014**, *4*, 1400025.

[S8] S. J. R. Prabakar, Y. H. Hwang, E. G. Bae, S. Shim, D. Kim, M. S. Lah, K. S. Sohn, M. Pyo, *Adv. Mater.* **2013**, *25*, 3307.

[S9] L. Wang, D. Wang, Z. H. Dong, F. X. Zhang, J. Jin, *Nano Lett.* **2013**, *13*, 1711.

[S10] S. Yang, W. Yue, J. Zhu, Y. Ren, X. J. Yang, *Adv. Funct. Mater.* **2013**, *23*, 3570.

[S11] J. Zhu, G. H. Zhang, X. Z. Yu, Q. H. Li, B. A. Lu, Z. Xu, *Nano Energy* **2014**, *3*, 80.

[S12] M. H. Wang, H. Yang, X. L. Zhou, W. Shi, Z. Zhou, P. Cheng, *Chem. Commun.* **2016**, *52*, 717.

[S13] X. S. Zhou, L. Yu, X. W. Lou, *Nanoscale* **2016**, *8*, 8384.

[S14] L. L. Fan, X. F. Li, B. Yan, J. M. Feng, D. B. Xiong, D. J. Li, L. Gu, Y. R. Wen, S. Lawes, X. L. Sun, *Adv. Energy Mater.* **2016**, 1502057.

[S15] J. Patra, H. C. Chen, C. H. Yang, C. T. Hsieh, C. Y. Su, J. K. Chang, *Nano Energy* **2016**, *28*, 124.

[S16] L. Pei, Q. Jin, Z. Zhu, Q. Zhao, J. Liang, J. Chen, *Nano Res.* **2015**, *8*, 184.

[S17] J. Yue, W. P. Wang, N. N. Wang, X. F. Yang, J. K. Feng, J. Yang, Y. T. Qian, *J. Mater. Chem. A* **2015**, *3*, 23194.

[S18] H.Z. Li, L.Y. Yang, 1, J. Liu, S.T. Li, L.B. Fang, Y.K. Lu, H.R. Yang, S.L. Liu, M. Lei, *J. Power Sources* **2016**, *324*, 780.

[S19] Y. Y. Cheng, J. F. Huang, J. Y. Li, Z. W. Xu, L. Y. Cao, H. Qi, *J. Power Sources* **2016**, *324*, 447.

[S20] R. S. Kalubarme, J. Y. Lee, C. J. Park, *ACS Appl. Mater. Interfaces* **2015**, *7*, 17226.